Strategies for enhancing quantum entanglement by local photon subtraction

Tim J. Bartley,[1,*] Philip J. D. Crowley,[1] Animesh Datta,[1] Joshua Nunn,[1] Lijian Zhang,[1,2] and Ian Walmsley[1]
[1]*Clarendon Laboratory, Department of Physics, University of Oxford, OX1 3PU Oxford, United Kingdom*
[2]*Max-Planck Institute for Structural Dynamics, University of Hamburg, 22607 Hamburg, Germany*
(Received 31 October 2012; published 13 February 2013)

Subtracting photons from a two-mode squeezed state is a well-known method to increase entanglement. We analyze different strategies of local photon subtraction from a two-mode squeezed state in terms of entanglement gain and success probability. We develop a general framework that incorporates imperfections and losses in all stages of the process: before, during, and after subtraction. By combining all three effects into a single efficiency parameter, we provide analytical and numerical results for subtraction strategies using photon-number-resolving and threshold detectors. We compare the entanglement gain afforded by symmetric and asymmetric subtraction scenarios across the two modes. For a given amount of loss, we identify an optimized set of parameters, such as initial squeezing and subtraction beam splitter transmissivity, that maximize the entanglement gain rate. We identify regimes for which asymmetric subtraction of different Fock states on the two modes outperforms symmetric strategies. In the lossless limit, subtracting a single photon from one mode always produces the highest entanglement gain rate. In the lossy case, the optimal strategy depends strongly on the losses on each mode individually, such that there is no general optimal strategy. Rather, taking losses on each mode as the only input parameters, we can identify the optimal subtraction strategy and required beam splitter transmissivities and initial squeezing parameter. Finally, we discuss the implications of our results for the distillation of continuous-variable quantum entanglement.

DOI: 10.1103/PhysRevA.87.022313 PACS number(s): 03.67.Bg, 42.50.Ex, 03.67.Hk, 03.67.Pp

I. INTRODUCTION

Efficient distribution of entanglement between distant parties is fundamental to most quantum communication protocols. However, entanglement is fragile and suffers from decoherence, which is detrimental to the performance of any communication protocol upon which it relies. The ability to increase the entanglement between communicating parties is therefore vital, and further, practical considerations dictate that this should be achieved through only local operations and classical communication (LOCC). While entanglement cannot increase *on average* under LOCC, a probabilistic protocol can be employed to increase the entanglement of a subset of states. This is the basis of entanglement distillation: extracting a small ensemble of more strongly entangled states from a larger ensemble of weakly entangled states [1].

In the discrete variable regime, entanglement distillation has been achieved using photonic qubits [2]. In the continuous-variable (CV) regime, the situation is more involved. Most common CV states and operations are Gaussian in nature. However, there exists a no-go theorem which states that one cannot distill entanglement from Gaussian states by Gaussian operations alone [3–5]. Gaussian operations are those with Hamiltonians which are (at most) quadratic in the ladder operators $\hat{a}$,$\hat{a}^\dagger$, comprising the basic tools of quantum optics, including beam splitters, phase shifters, squeezers, and homodyne detection. A number of protocols to increase entanglement in CV systems have been proposed [6–11], elements of which have been implemented [12–16].

Photon subtraction was initially proposed by Opatrný *et al.* to increase the efficacy of a teleportation protocol [6]. Since then, several studies have looked at photon subtraction in more detail. Cochrane *et al.* investigated subtracting and detecting n photons simultaneously from the modes of a two-mode squeezed state [17]. Olivares *et al.* studied the use of on-off (single-photon threshold) detectors to measure at least one photon subtracted from both modes coincidentally, again in terms of the improvement of a teleportation protocol [18]. Kitagawa *et al.* provided a detailed numerical analysis of two-mode subtraction by on-off detectors in terms of the explicit change in entanglement and compared this with the operational measures used previously in the literature [19]. This work was built on by Zhang and van Loock [20] in which analytical results for perfect symmetric subtraction using photon-number-resolving detectors and on-off detectors were derived. More recently, Navarrete-Benlloch *et al.* extended the analysis to asymmetric subtraction and quantified the non-Gaussianity of the operations [21]. Photon subtraction (and addition) is discussed more generally in terms of quantum-state engineering in the review by Kim [22] and in terms of non-Gaussian entanglement quantification in Ref. [23]. Experimentally, both nonlocal [24] and local [16] photon subtraction from two-mode squeezed states have been demonstrated.

In this paper, we extensively investigate the best entanglement enhancement strategy in a realistic experimental scenario. We present practical figures of merit based on the entanglement gain and success probability of photon subtraction protocols. Using the log negativity [25] as an entanglement metric allows us to quantify the entanglement of mixed states caused by losses. Indeed, we consider six independent loss parameters and allow for detecting different numbers of photons subtracted from each mode, which we refer to as asymmetric subtraction. In addition, our model considers both on-off and photon-number-resolving detectors to measure the subtracted photons. Our results can be applied directly to realistic experiments, as well as providing a

*t.bartley1@physics.ox.ac.uk

framework in which to study other entanglement-enhancing strategies.

This article is organized as follows: in Sec. II, we define the figures of merit by which protocols that increase entanglement may be measured. In Sec. III, we derive the state evolution of photon subtraction from a two-mode squeezed state (TMSS), and we provide an analytical form for the probabilities corresponding to different detection strategies. We use the evolved state to analyze the gain in entanglement by different subtraction strategies: using photon-number-resolving detectors (PNRDs) in Sec. IV and threshold detectors (such as avalanche photodiodes, APDs) in Sec. V. For both types of detectors (PNRDs in Sec. IV D and APDs in Sec. V C), we numerically analyze symmetric and asymmetric subtraction in the presence of loss occurring before, during, and after subtraction and show how these different parameters affect the success of the protocol. We also list the main conclusions drawn from our work in Sec. VI.

II. ENTANGLEMENT, GAIN, AND RATE

Entanglement in this system can be captured conveniently by the positive partial transpose (PPT) criterion. If the partial transpose ρ^{T_A} of a density matrix ρ has negative eigenvalues, then ρ must be entangled [26,27]. The sum of the absolute values of the negative eigenvalues of ρ^{T_A} is defined as the negativity $N(\rho)$. The entanglement measure we use in this paper is the log negativity [25], defined as

$$E_N(\rho) = \log_2[1 + 2N(\rho)] = \log_2 ||\rho^{T_A}||_1, \tag{1}$$

where $||X||_1 = \mathrm{Tr}\left[\sqrt{X^\dagger X}\right]$ denotes the trace norm of X.

The maximally entangled CV state, for a fixed energy, is the TMSS, as generated during parametric down conversion (PDC) or, equivalently, by interfering two single-mode squeezed vacua in phase at a 50:50 beam splitter [28]. This state can be written in the Fock basis as

$$|\psi_{\mathrm{TMSS}}\rangle = \sqrt{1-\lambda^2}\sum_{n=0}^{\infty}\lambda^n|n,n\rangle_{AA'} \tag{2a}$$

$$= \sqrt{1-\lambda^2}\sum_{n=0}^{\infty}\frac{\lambda^n}{n!}a^{\dagger n}a'^{\dagger n}|0,0\rangle_{AA'}, \tag{2b}$$

which describes n pairs of photons in modes A and A' for a given squeezing parameter $\lambda \in [0,1)$, and we define $|n,m\rangle_{AA'} = |n\rangle_A \otimes |m\rangle_{A'}$.

The density matrix of this state is

$$\rho_{\mathrm{TMSS}} = (1-\lambda^2)\sum_{n=0}^{\infty}\sum_{m=0}^{\infty}\lambda^n\lambda^m|n\rangle_A\langle m| \otimes |n\rangle_{A'}\langle m|, \tag{3}$$

the partial transpose (with respect to mode A) of which is

$$\rho_{\mathrm{TMSS}}^{T_A} = (1-\lambda^2)\sum_{n=0}^{\infty}\sum_{m=0}^{\infty}\lambda^n\lambda^m|m\rangle_A\langle n| \otimes |n\rangle_{A'}\langle m|. \tag{4}$$

Taking the trace norm yields

$$\left|\left|\rho_{\mathrm{TMSS}}^{T_A}\right|\right|_1 = (1-\lambda^2)\mathrm{Tr}\left[\sum_{n=0}^{\infty}\lambda^n|n\rangle\langle n|\right]\mathrm{Tr}\left[\sum_{m=0}^{\infty}\lambda^m|m\rangle\langle m|\right]$$
$$= \frac{(1-\lambda^2)}{(1-\lambda)^2}; \tag{5}$$

therefore the TMSS defined in Eq. (2a) has log negativity

$$E_N(\rho_{\mathrm{TMSS}}) = \log_2\left(\frac{1+\lambda}{1-\lambda}\right), \tag{6}$$

which is the benchmark against which changes in entanglement will be measured.

From this initial state ρ_{TMSS}, a subtraction step $\mathfrak{s}$ produces a state $\rho_{\mathfrak{s}}$ with entanglement $E_N(\rho_{\mathfrak{s}})$. We define the *gain* in entanglement $G(\rho_{\mathfrak{s}})$ as the difference between entanglement after distillation and that of the initial state, normalized to the initial entanglement, i.e.,

$$G(\rho_{\mathfrak{s}}) = \frac{E_N(\rho_{\mathfrak{s}})}{E_N(\rho_{\mathrm{TMSS}})} - 1, \tag{7}$$

such that $G(\rho_{\mathfrak{s}}) > 0$ if the subtraction step increases entanglement.

The probability of an entanglement-enhancing step must be less than unity since entanglement cannot be increased on average under LOCC [29]. It is calculated by

$$P(\rho_{\mathfrak{s}}) = \mathrm{Tr}[\mathfrak{s}(\rho)], \tag{8}$$

where $\mathfrak{s}(\rho)$ is the unnormalized density matrix following a subtraction operation. The final density matrix $\rho_{\mathfrak{s}}$ is found by normalizing $\mathfrak{s}(\rho)$ as follows:

$$\rho_{\mathfrak{s}} = \frac{\mathfrak{s}(\rho)}{\mathrm{Tr}[\mathfrak{s}(\rho)]}. \tag{9}$$

The aim of an entanglement enhancement protocol is to increase entanglement from some initial value. It is therefore desirable not only for subtraction to produce a high gain but also to do so at a high rate, i.e., that the probability of a subtraction event is as high as possible. In general these conditions cannot be met independently; therefore there exists an optimum to be found based on the parameters of a given implementation. We therefore define the *entanglement gain rate* (frequently shortened to "rate" in the remainder of the paper) $\Gamma(\rho_{\mathfrak{s}})$ as the gain afforded by a distillation step $G(\rho_{\mathfrak{s}})$ multiplied by its likelihood,

$$\Gamma(\rho_{\mathfrak{s}}) = P(\rho_{\mathfrak{s}})\,G(\rho_{\mathfrak{s}}). \tag{10}$$

By postselecting on successful subtraction events, the entanglement of this subensemble can be increased. The increase will depend on the parameters of the subtraction step employed and can be maximized to determine the values of those parameters which yield the highest rate.

III. THE PROTOCOL

To effect subtraction and account for loss, we consider an array of eight beam splitters, each with transmissivity T_i and reflectivity $R_i = \sqrt{1-T_i^2}$, acting on the TMSS as shown in Fig. 1. The state initially occupies modes A, A'. The beam splitters T_2, T_2' effect subtraction, while the other beam

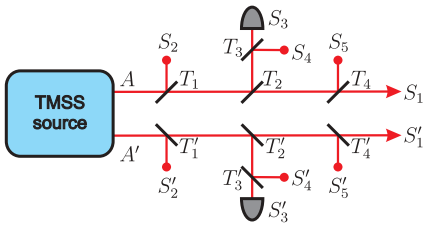

FIG. 1. (Color online) A TMSS in a photon-subtraction setup. A TMSS initially occupies modes A,A'. Following the array of beam splitters (with transmissivity T_i,T_i'), we seek the entanglement in modes S_1,S_1' following detection in modes S_3,S_3'. Losses are modeled by photons in modes before (S_2,S_2'), during (S_4,S_4'), and after (S_5,S_5') detection.

splitters T_1,T_3,T_4 model losses before subtraction, during detection, and after subtraction, respectively (and similarly for the primed counterparts). As such, the state vector describing the combined state of the input modes may be written $|\Psi_{\text{in}}\rangle = |\psi_{\text{TMSS}}\rangle \otimes |0\rangle^{\otimes 8}$. The evolution of the input modes is governed by the unitary transformation $U \oplus U'$. The unitaries U and U' actually denote the orthogonal (rotation) matrices corresponding to symplectic transformations in the Heisenberg picture and operate on the modes as labeled in Fig. 1 and circuit diagram (13). The elements of U,U' depend on the arrangement of beam splitters and how they couple their respective modes. For the array of beam splitters shown in Fig. 1, U may be written as

$$U=\begin{pmatrix} T_1T_2T_4 & -R_1T_2T_4 & -R_2T_4 & 0 & -R_4 \\ R_1 & T_1 & 0 & 0 & 0 \\ T_1R_2T_3 & -R_1R_2T_3 & T_2T_3 & -R_3 & 0 \\ T_1R_2R_3 & -R_1R_2R_3 & T_2R_3 & T_3 & 0 \\ T_1T_2R_4 & -R_1T_2R_4 & -R_2R_4 & 0 & T_4 \end{pmatrix} \tag{11}$$

and similarly for U', with all symbols replaced by their primed counterparts. Since the only nonvacuum input modes are A,A', the output modes depend only on the first column of each component unitary U,U'. Indeed, we may write the output state vector in the Fock basis as

$$|\Psi_{\text{out}}\rangle = \sqrt{1-\lambda^2}\sum_{n=0}^{\infty}\frac{\lambda^n}{n!}\left(\sum_{m=1}^{5}\sigma_{1,m}s_m^\dagger\right)^n \times\left(\sum_{m'=1}^{5}\sigma'_{1,m'}s_{m'}'^\dagger\right)^n|0\rangle, \tag{12}$$

where $\sigma_{1,m}$ is the $(1,m)$th element of the unitary U and $s_m^\dagger$ is the creation operator for the mode m. We are interested in the entanglement between the modes S_1,S_1', occupied by e,e' photons, respectively, dependent on detecting d,d' photons in modes S_3,S_3', respectively. The modes $S_2,S_4,S_5,S_2',S_4',S_5'$ contain l,l' photons lost to the environment. These loss modes can be combined, simplifying our problem into the following circuit diagram:

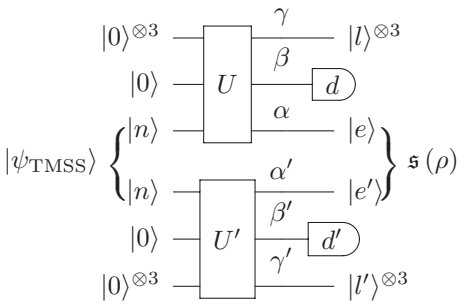

(13)

The photons in two input modes of the TMSS are divided into three output modes each: entangled, detected, and lost, and we assign parameters α,α', β,β', and γ,γ' to be the fraction of photons in each mode, respectively. These may be written in terms of the components of the unitary U as follows:

$$\alpha^2 \equiv \sigma_{1,1}^2 = T_1^2T_2^2T_4^2, \tag{14a}$$

$$\beta^2 \equiv \sigma_{1,3}^2 = T_1^2R_2^2T_3^2, \tag{14b}$$

$$\gamma^2 \equiv \sum_{m=2,4,5}\sigma_{1,m}^2 = R_1^2 + T_1^2\left(R_2^2R_3^2 + T_2^2R_4^2\right), \tag{14c}$$

where the coefficients satisfy $\alpha^2+\beta^2+\gamma^2=1$, as defined by the unitarity condition (and similarly for their primed counterparts). Substituting Eqs. (14) into Eq. (12) yields

$$|\Psi_{\text{out}}\rangle = \sqrt{1-\lambda^2}\sum_{n=0}^{\infty}\lambda^n\sum_{\mathcal{S}}c_{e,d,l}c'_{e',d',l'}|e,e'\rangle|d,d'\rangle|l,l'\rangle, \tag{15}$$

where the summation is over $\mathcal{S}=\{e,e',d,d',l,l'$ subject to $e+d+l=e'+d'+l'=n\}$ and where we have defined

$$c_{e,d,l} = \sqrt{\binom{n}{e,d,l}}\alpha^e\beta^d\gamma^l, \tag{16}$$

with the multinomial coefficient [30] $\binom{n}{e,d,l}$ (and similarly for the primed quantities). On tracing out the loss and detected modes, we obtain the (mixed) entangled state ρ across modes S_1,S_1' as

$$\rho = (1-\lambda^2)\sum_{n,\tilde{n}=0}^{\infty}\sum_{d,d'}^{d_{\max},d'_{\max}}\sum_{l,l'}^{l_{\max}}c_{n,\tilde{n},d,d',l,l'}|e\rangle_{S_1}\langle\tilde{e}|\otimes|e'\rangle_{S_1'}\langle\tilde{e}'|, \tag{17}$$

where $d_{\max}=\min(n,\tilde{n})-l$, $l_{\max}=\min(n,\tilde{n})$, and $c_{n,\tilde{n},d,d',l,l'}$ are subject to the constraints $e+d+l=e'+d'+l'=n,\tilde{e}+d+l=\tilde{e}'+d'+l'=\tilde{n}$, such that

$$c_{n,\tilde{n},d,d',l,l'} = \frac{\lambda^{n+\tilde{n}}n!\tilde{n}!\alpha^{e+\tilde{e}}\alpha'^{e'+\tilde{e}'}\beta^{2d}\beta'^{2d'}\gamma^{2l}\gamma'^{2l'}}{d!d'!l!l'!\sqrt{e!e'!\tilde{e}!\tilde{e}'!}}. \tag{18}$$

As the mode structure is now clear, we will suppress the mode labels S_1,S_1' in further discussions for compactness.

A. Subtraction

Subtraction is effected by changing the limits of the summation over d,d' in Eq. (17), leading to an unnormalized subtracted state $\mathfrak{s}(\rho)$. The exact form of this state depends on

the subtraction strategy employed and is derived in detail in the relevant sections below. To calculate the entanglement we seek the sum of the negative eigenvalues of the partial transpose of the normalized state. Using Eqs. (1) and (9), we therefore seek

$$E_n(\rho_{\mathfrak{s}}) = \log_2\left\{\frac{||\mathfrak{s}(\rho)^{T_{S_1}}||_1}{\mathrm{Tr}[\mathfrak{s}(\rho)]}\right\}, \tag{19}$$

where $\mathfrak{s}(\rho)^{T_{S_1}}$ is the partially transposed unnormalized state with respect to mode S_1. Following the analysis in Refs. [19, 20], we can write $\mathfrak{s}(\rho)^{T_{S_1}}$ in block diagonal form, and we change variables such that

$$n \equiv i+l+d, \quad \tilde{n} \equiv j+l+d, \quad l' \equiv i+j-K+l+d-d', \tag{20}$$

where the indices i,j denote the rows and columns of the Kth block matrix of dimension $K+1$. Thus $\mathfrak{s}(\rho)^{T_{S_1}}$ is written explicitly as

$$\mathfrak{s}(\rho)^{T_{S_1}} = (1-\lambda^2)\bigoplus_{K=0}^{\infty}\sum_{i,j=0}^{K} C_{i,j}^{(K)}|j\rangle\langle i| \otimes |K-i\rangle\langle K-j|, \tag{21}$$

with coefficients

$$C_{i,j}^{(K)} = \sum_{d,d'=t,t'}^{t_{\max},t'_{\max}}\sum_{l=l_0}^{\infty}\frac{\lambda^{i+j+2(l+d)}\alpha^{i+j}\alpha'^{2K-i-j}\beta^{2d}\beta'^{2d'}\gamma^{2l}\gamma'^{2(i+j-K+l+d-d')}(i+l+d)!\,(j+l+d)!}{l!\,(l+i+j+d-K-d')!d!d'!\sqrt{i!\,j!\,(K-j)!\,(K-i)!}}, \tag{22}$$

where $l_0 = \max\{0, K+d'-d-i-j\}$ and $t,t',t_{\max},t'_{\max}$ depend on the type of detector employed. By inspection the matrices $\mathbf{C}^{(K)} = [C_{i,j}^{(K)}]_{i=0,\ldots,K;j=0,\ldots,K}$ are symmetric, and they are also persymmetric (and therefore centrosymmetric) when the primed parameters are equal to their unprimed counterparts and the range of the summations over d and d' are equal [20]. Equation (22) is central to the derivation of all subsequent analytic results.

The coefficients $C_{i,j}^{(K)}$ lead to a normalized state if d,d' are summed over entirely, i.e., the limits on the summation over d,d' are $t=t'=0, t_{\max}=t'_{\max}=\infty$, respectively. The (unnormalized) state $\mathfrak{s}(\rho)$ following a subtraction event is found by placing limits on the d,d' summation, yielding coefficients $\tilde{C}_{i,j}^{(K)} = C_{i,j}^{(K)}(t,t',t_{\max},t'_{\max})$, dependent on the strategy employed. For threshold detectors that click on receipt of a minimum number of photons, the sum runs from the threshold value t to $t_{\max}=\infty$ (for instance, single-photon avalanche detectors have $t=1$). For PNRDs operating within their resolution regime, the summation disappears since $t_{\max}=t$.

IV. SUBTRACTION USING PNRDs

We will first briefly consider the case when subtracted photons are measured using perfect PNRDs. This amounts to removing the sums over d,d' in Eq. (22).

A. Probability of photon subtraction

The probability $P(t,t') = P(\rho_{\mathfrak{s}})$ of detecting $t=t_{\max}$, $t'=t'_{\max}$ photons, respectively, is given by the trace of the unnormalized state $\mathfrak{s}(\rho)$ after a subtraction event. Detecting t,t' subtracted photons by PNRDs projects onto modes S_1,S_1' the unnormalized state

$$\mathfrak{s}(\rho) = (1-\lambda^2)\bigoplus_{K=0}^{\infty}\sum_{i,j=0}^{K}\tilde{C}_{i,j}^{(K)}|i\rangle_E\langle j| \otimes |K-i\rangle_{E'}\langle K-j|, \tag{23}$$

where the coefficients $\tilde{C}_{i,j}^{(K)} = C_{i,j}^{(K)}(t,t',t,t')$ are identical to those in Eq. (22) for $t_{\max}=t, t'_{\max}=t'$, and therefore the summation over d is dropped. This has probability

$$P(t,t') = \mathrm{Tr}[\mathfrak{s}(\rho)] = \frac{(1-\lambda^2)\lambda^{2t'}\beta'^{2t'}\beta^{2t}(\alpha^2+\gamma^2)^{t'-t}}{[1-(\alpha^2+\gamma^2)(\alpha'^2+\gamma'^2)\lambda^2]^{t'+1}} \times P_t^{(t'-t,0)}\left[\frac{1+(\alpha^2+\gamma^2)(\alpha'^2+\gamma'^2)\lambda^2}{1-(\alpha^2+\gamma^2)(\alpha'^2+\gamma'^2)\lambda^2}\right], \tag{24}$$

where $P_n^{(a,b)}[z]$ denotes the nth-order Jacobi polynomial. We have assumed, without loss of generality, that $t \leqslant t'$; owing to the symmetry of the problem a corresponding equation for $t \geqslant t'$ can be found by swapping all of the primed values with their unprimed counterparts. This expression is valid if t,t' are known, i.e., in the case where detection resolves photon number. This may be extended to threshold detectors by summing over t,t' from the threshold $\tilde{t},\tilde{t}'$ (typically unity) to $t_{\max},t'_{\max}$. We deal with this scenario in greater detail in Sec. V.

B. Lossless symmetric subtraction

Perfect symmetric photon subtraction detects an equal number of photons in both modes with 100% efficiency. This is equivalent to setting $\gamma=\gamma'=0$, whereby $l=l'=0$ and $\alpha=T_2$, the transmissivity of the subtraction beam splitter. Symmetry implies $t=t'$, $\alpha=\alpha'$, and $\beta=\beta'$, implying $K=i+j$, which simplifies Eq. (22) to

$$C_{i,j}^{(K)} = \frac{\lambda^{K+2t}\alpha^{2K}\beta^{4t}(i+t)!\,(j+t)!}{t!^2\sqrt{i!\,j!\,(K-i)!\,(K-j)!}}\delta_{K,i+j}, \tag{25}$$

where the Kronecker delta function $\delta_{K,i+j}$ means that all off-antidiagonal elements are zero. In this case, each of the $(K+1)\times(K+1)$ blocks $\mathbf{C}^{(K)}$ are both symmetric, $C_{i,j}^{(K)} = C_{j,i}^{(K)}$, and persymmetric, $C_{i,j}^{(K)} = C_{K-i,K-j}^{(K)}$, which can be exploited [20,31] to compute the log negativity using

$$E_N(\rho) = \log_2\left\{\frac{(1-\lambda^2)\sum_{K=0}^{\infty}\mathrm{Tr}[\mathbf{J}^{(K)}\mathbf{C}^{(K)}]}{P(t,t)}\right\}, \tag{26}$$

where $\mathbf{J}^{(K)} = [\delta_{i+j,K}]$ is the anti-identity matrix and we include explicitly the normalization factor in the denominator.

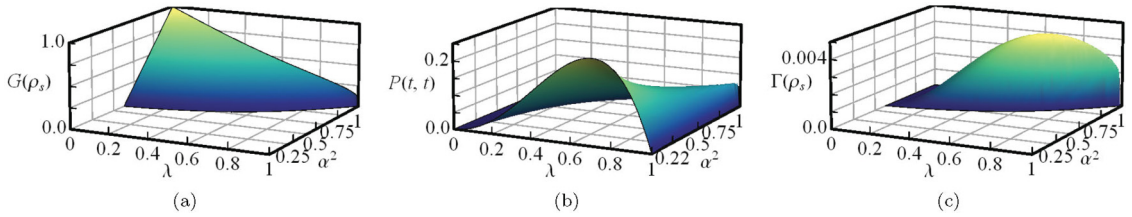

FIG. 2. (Color online) Lossless symmetric subtraction of a single photon using perfect photon-number-resolving detectors. (a) Entanglement gain, (b) distillation probability, and (c) rate are shown for $\lambda \in [0,1)$ and $\alpha^2 \in [0,1)$.

The numerator traces over the antidiagonal elements $C^{(K)}_{i,K-i}$, while the denominator traces over the diagonal elements $C^{(K)}_{i,i}$. This yields

$$\sum_{K=0}^{\infty} \mathrm{Tr}[\mathbf{J}^{(K)}\mathbf{C}^{(K)}]$$
$$= (\lambda\beta^2)^{2d} \sum_{K=0}^{\infty}\sum_{i=0}^{K} (\lambda\alpha^2)^K \frac{(i+t)!\,(K-i+t)!}{t!^2 i!\,(K-i)!}$$
$$= \left(\frac{\lambda\beta^2}{1-\lambda\alpha^2}\right)^{2t} \frac{1}{\left(1-\lambda\alpha^2\right)^2}, \tag{27}$$

and from Eq. (24), the probability simplifies to

$$P\,(t,t) = \frac{(1-\lambda^2)\lambda^{2t}\beta^{4t}}{(1-\lambda^2\alpha^4)^{t+1}} P_t\left[\frac{1+(\lambda\alpha^2)^2}{1-(\lambda\alpha^2)^2}\right], \tag{28}$$

where $P_n[z]$ is the nth Legendre polynomial, a special case of the Jacobi polynomial $P_n^{(a,b)}[z]$ found in Eq. (24) given by $P_n^{(0,0)}[z] = P_n[z]$. This is an analytic, closed-form expression of the results in Refs. [19,20] and yields an entanglement of

$$E_N\,(\rho_{\mathfrak{s}}) = \log_2\left\{\left(\frac{1+\lambda\alpha^2}{1-\lambda\alpha^2}\right)^{t+1} \Big/ P_t\left[\frac{1+(\lambda\alpha^2)^2}{1-(\lambda\alpha^2)^2}\right]\right\}. \tag{29}$$

Figure 2 depicts the result for varying squeezing parameter λ and subtraction coefficient α^2. The behavior of the entanglement gain rate in Fig. 2(c) shows that there exists an optimum value that provides the best entanglement yield per trial. High gain is less likely, such that the rate is peaked at particular values of $\lambda_{\mathrm{opt}} = 0.66$ and $\alpha^2_{\mathrm{opt}} = 0.83$. On average, these parameters produce the highest gain in entanglement per trial.

In general, the parameter α^2 is freely tunable when performing the protocol, whereas λ is restricted by the maximum squeezing available. Therefore it is useful to obtain an expression for the optimal subtraction parameter α^2_{opt} in terms of the initial squeezing λ that maximizes the entanglement gain rate $\Gamma\,(\rho_{\mathfrak{s}})$. These values are obtained from Fig. 2(c) and are plotted as a function of λ in Fig. 3(a). For $t = 1$, the fit to these data is a second-order polynomial of the form

$$\alpha^2_{\mathrm{opt}} = 0.238\,(\lambda-1)^2 + 0.576\,(\lambda-1) + 1. \tag{30}$$

Thus, given that in the lossless case $\alpha = T_2$, we have the recipe to dial up the most effective subtraction rate to maximize the gain in entanglement per trial.

It has been shown previously that, all things being equal, subtracting more photons increases the gain after subtraction [20]. However, by optimizing α^2 with respect to the rate, this gain is only marginally higher with increasing d, as shown in Fig. 3(c). Indeed, at $\lambda > 0.6$, there is no advantage

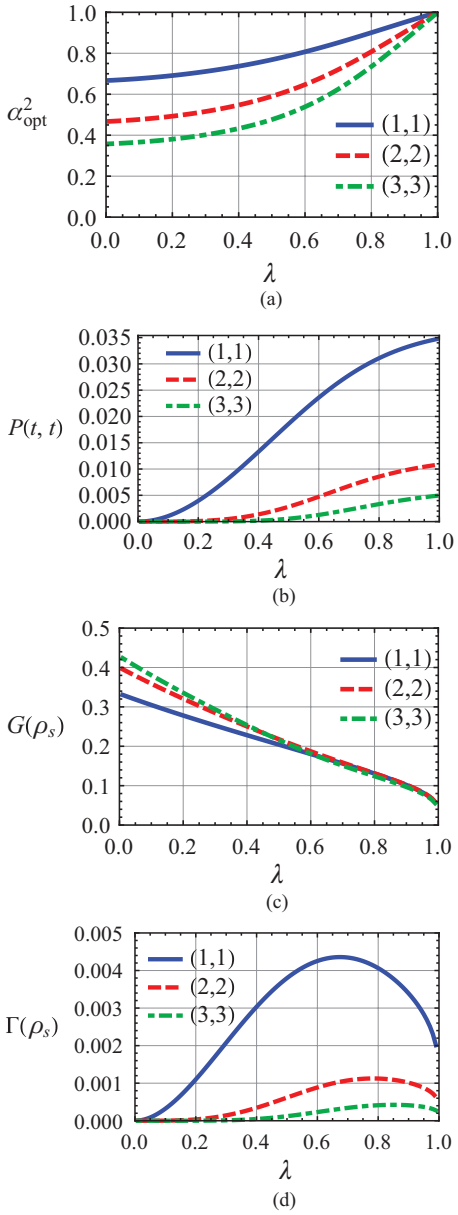

FIG. 3. (Color online) Lossless symmetric subtraction with PNRDs. 3(a) α^2 optimized over entanglement gain rate for a given λ for different numbers of subtracted photons t. The maximum (b) probability, (c) gain, and (d) rate achieved with the optimal α^2 as a function of λ for different values of t.

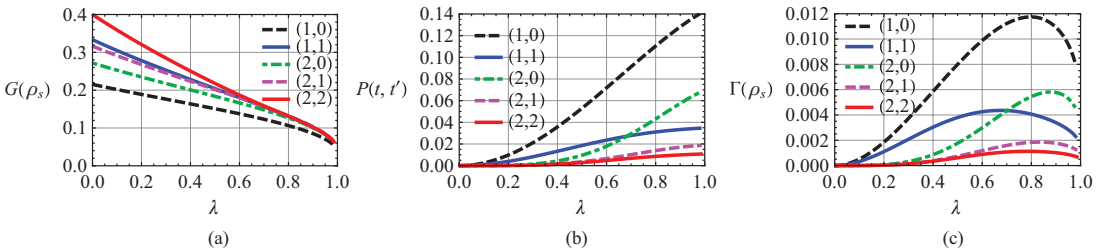

FIG. 4. (Color online) Lossless symmetric and asymmetric subtraction with PNRDs. Using α,α' optimized over entanglement gain rate for different combinations of subtracted photons ($t,t' \leqslant 2$), we calculate (a) the achievable gain, (b) the success probability, and (c) entanglement gain rate as a function of λ.

to subtracting more photons. As expected, even with the optimal α^2, the probability of entanglement gain decreases significantly with increasing t, shown in Fig. 3(b). These effects combine to yield a lower entanglement gain rate as the number of subtracted photons is increased, as shown in Fig. 3(d).

C. Lossless asymmetric subtraction

We now consider the case of perfect *asymmetric* subtraction, i.e., detecting different numbers of photons $t \neq t'$ in each subtracted mode. When counting resources in terms of total photons subtracted, asymmetric subtraction allows us to double our space to include odd photon numbers. This additional degree of freedom lifts the degeneracy in the coefficients, i.e., the primed quantities may take different values from their unprimed counterparts. This doubles the number of parameters over which the protocol can be optimized.

Starting again from Eq. (22), we detect t,t' photons in each mode with unit efficiency. Since we are neglecting the effects of loss in the system, $\gamma = \gamma' = 0$, and as such the only nonzero contribution to the summation over l is the $l = 0$ term. Photon-number resolution is maintained by setting $t_{\max} = t, t'_{\max} = t'$ in Eq. (22) as before; however, they need not be equal as in the case above. In this scheme the relation $\gamma = \gamma' = 0$ ensures that all elements of $\mathbf{C}^{(K)}$, except those that satisfy $i + j = K + t' - t$, are zero. We may thus express the elements of $\mathbf{C}^{(K)}$ as

$$C^{(K)}_{i,j} = (1-\lambda^2)\lambda^{i+j+2t}\alpha^{i+j}\alpha'^{2K-i-j}\beta^{2t}\beta'^{2t'} \times \frac{(i+t)!(j+t)!}{t!t'!\sqrt{i!j!(K-i)!(K-j)!}}\delta_{i+j,K+t'-t}. \quad (31)$$

The matrices $\mathbf{C}^{(K)}$ only have elements along one of their skew diagonals, shifted from the main skew diagonal by $t'-t$. This allows us to define an antidiagonal submatrix $\mathbf{B}^{(\bar{K})}$, where $\mathbf{B}^{(\bar{K})}$ is a $(\bar{K}+1)\times(\bar{K}+1)$ matrix and where $\bar{K} = K - t' + t$, which contains the elements on its main skew diagonal. Without loss of generality, we are able to choose $t \leqslant t'$, whereby the elements of $\mathbf{B}^{(\bar{K})}$ are $B^{(\bar{K})}_{i,j} = C^{(K)}_{i+t'-t,j+t'-t}$. This is both symmetric and persymmetric, so the above approach can again be used in computing the negativity. When evaluating $\mathrm{Tr}[\mathbf{B}^{(\bar{K})}\mathbf{J}^{(\bar{K})}]$, the elements of interest are $B^{(\bar{K})}_{i,\bar{K}-i} = C^{(K)}_{i+t'-t,K-i}$, where

$$B^{(\bar{K})}_{i,\bar{K}-i} = (1-\lambda^2)\lambda^{\bar{K}+2t'}\alpha^{\bar{K}+2(t'-t)}\alpha'^{\bar{K}}\beta^{2t}\beta'^{2t'} \times \frac{(i+t')!(\bar{K}-i+t')!}{t!t'!\sqrt{(i+t'-t)!(\bar{K}-i+t'-t)!(\bar{K}-i)!i!}}. \quad (32)$$

Equations (24) and (32) together lead to the relations

$$P(t,t') = \frac{(1-\lambda^2)\lambda^{2t'}\beta'^{2t'}\beta^{2t}\alpha^{2(t'-t)}}{(1-\alpha^2\alpha'^2\lambda^2)^{t'+1}} \times P_t^{(t'-t,0)}\left[\frac{1+(\alpha\alpha'\lambda)^2}{1-(\alpha\alpha'\lambda)^2}\right] \quad (33)$$

and

$$\sum_{\bar{K}=0}^{\infty}\mathrm{Tr}[\mathbf{B}^{(\bar{K})}\mathbf{J}^{(\bar{K})}] = (1-\lambda^2)(\lambda\beta')^{2t'}\beta^{2t}\alpha^{2(t'-t)} \times \left(\sum_{i=0}^{\infty}(\lambda\alpha\alpha')^i\frac{(i+t')!}{\sqrt{i(i+t'-t)!t!t'}}\right)^2. \quad (34)$$

Unfortunately, no analytical expression could be found for the sum of series in brackets. However, by considering the ratios between successive terms in the series, it is clear that it converges over the relevant range $0 < \lambda\alpha\alpha' < 1$. This gives an exact, but not closed, form for the log negativity of the state

$$E_N(\rho_s) = \log_2\left\{\frac{(1-\alpha^2\alpha'^2\lambda^2)^{t'+1}}{P_t^{(t'-t,0)}\left[\frac{1+\alpha^2\alpha'^2\lambda^2}{1-\alpha^2\alpha'^2\lambda^2}\right]}\right\} + 2\log_2\left\{\sum_{i=0}^{\infty}(\lambda\alpha\alpha')^i\frac{(i+t')!}{\sqrt{i!\,(i+t'-t)!t!t'!}}\right\}. \quad (35)$$

1. Comparing symmetric and asymmetric subtraction

As with the symmetric case earlier, we can directly compare the entanglement gain, probability, and rate for asymmetric subtraction. For illustration purposes, we compare different ways of subtracting up to two photons from each mode. The results are shown in Fig. 4.

It is clear from Fig. 4(a) that the symmetric cases, $(t,t') = (1,1)$ and $(2,2)$, produce more gain than their asymmetric counterparts for a fixed number of subtracted photons. From

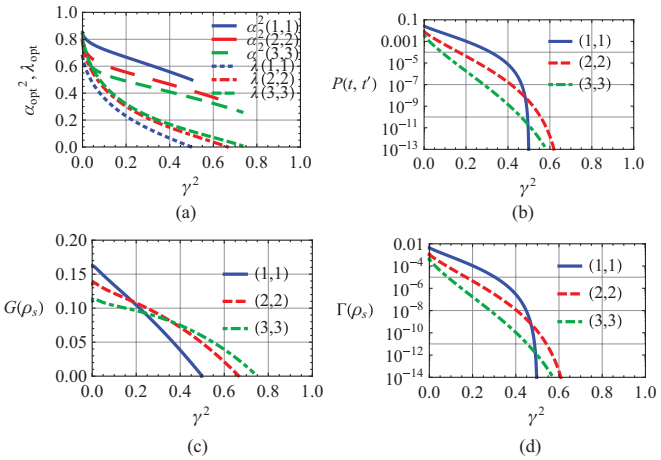

FIG. 5. (Color online) Lossy symmetric subtraction with PNRDs. (a) Squeezing λ and subtraction α^2 parameters, optimized to produce the highest entanglement gain rate at a given loss and the resulting (b) probability, (c) gain, and (d) rate resulting from these parameters.

Fig. 4(b), there exists a regime of $\lambda \gtrsim 0.7$ for which the probability of subtracting (2,0) photons is greater than the (1,1) case; therefore the gain rate, shown in Fig. 4(c), is correspondingly higher in this regime. This is because the (2,0) subtraction event is more likely than the (1,1) case for high values of λ. However, it is clear that in general the asymmetric (1,0) case produces the most entanglement gain per trial, once again due to the high likelihood of subtracting 1 photon as opposed to 2 photons in any combination.

D. Losses and imperfect detection

In any realistic scenario, where the process of entanglement distillation and entanglement enhancement will be most essential, the detectors are imperfect, and evolving quantum states suffer losses. Losses are accounted for by setting $\gamma,\gamma' > 0$, and the summation over l (which denotes the number of photons lost) includes contributions from $l \geqslant 1$ which are nonzero. Losses are modeled by beam splitters before, during, and after subtraction, as shown in Fig. 1. The effect of loss, for the symmetric cases where one [blue (dark gray)], two [red (medium gray)] and three [green (light gray)] photons are detected from each mode, is shown in Fig. 5. As the combined loss γ^2 increases, optimal initial squeezing λ for which entanglement can be enhanced by local photon subtraction decreases. Furthermore, detecting higher numbers of photons is more loss tolerant; since a smaller α^2 is required to subtract more photons, the restriction on $\gamma^2 \leqslant 0.5$ is reduced. Indeed, we can define $\gamma^2_{\max}$ as the maximum loss for which entanglement still increases on subtraction. The dependence of the maximum losses $\gamma_{\max} = 1/t + 1$ comes from the gain as a function of loss, setting to zero and solving for t the difference of Eqs. (6) and (38).

The constituents of γ,γ' are determined by Eq. (14c), where we define efficiencies before, during, and after detection as T_1^2, T_3^2, and T_4^2, respectively. From the expressions of γ,γ', it is clear that each of these efficiencies contribute differently to losses. The effect of detector efficiency, parameterized by T_3, is almost negligible. This can be interpreted by considering the subtraction detector as something of a postselector: it may not often click, but when it does, one can be fairly certain that entanglement has been increased. Losses after subtraction may be mitigated in a similar way, by using a loss-tolerant entanglement detection strategy, such as postselection or a loss-tolerant entanglement witness [32]. Loss before subtraction, which may be modeled as a mixing of the state due to nonunit channel transmission, is unavoidable, and its contribution is significant.

1. Entanglement gain and rate under loss

To study the enhancement of entanglement in the presence of losses and imperfection, we again start from Eq. (22), which in the symmetric detection PNRD case for $t = t'$ is given by

$$C_{i,j}^{(K)} = \sum_{l=l_0}^{\infty} \lambda^{i+j+2(t+l)} \alpha^{2K} \beta^{4t} \gamma^{2(i+j-K+2l)} \times \frac{(i+l+t)!\,(j+l+t)!}{l!\,(l+i+j-K)!\,t!^2 \sqrt{i!\,j!\,(K-j)!\,(K-i)!}}, \tag{36}$$

where $l_0 = \max(0, K-i-j)$. Since this matrix is symmetric and persymmetric, we can calculate the entanglement following [20]. Defining $x = 1-\alpha^2\lambda$ and $y = (\alpha^2+\gamma^2)\lambda$ allows us to write

$$\mathrm{Tr}[\mathbf{J}^{(\mathrm{K})}\mathbf{C}^{(\mathrm{K})}] = \frac{(1-\lambda^2)\beta^{4t}\lambda^{2t}}{(x^2-\gamma^4\lambda^2)^{t+1}} P_t\left[\frac{x^2+\gamma^4\lambda^2}{x^2-\gamma^4\lambda^2}\right],$$

and the success probability is given by

$$P(t,t) = \frac{(1-\lambda^2)\beta^{4t}\lambda^{2t}}{[1-y^2\lambda^2]^{t+1}} P_t\left[\frac{1+y^2}{1-y^2}\right]. \tag{37}$$

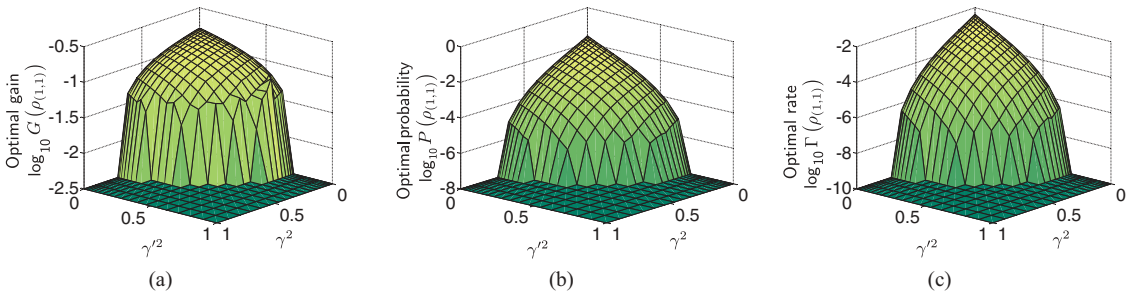

FIG. 6. (Color online) Lossy symmetric subtraction with PNRDs. The (a) gain, (b) probability, and (c) rate of entanglement increase as a function of loss γ^2, γ'^2, given one photon subtracted from each mode.

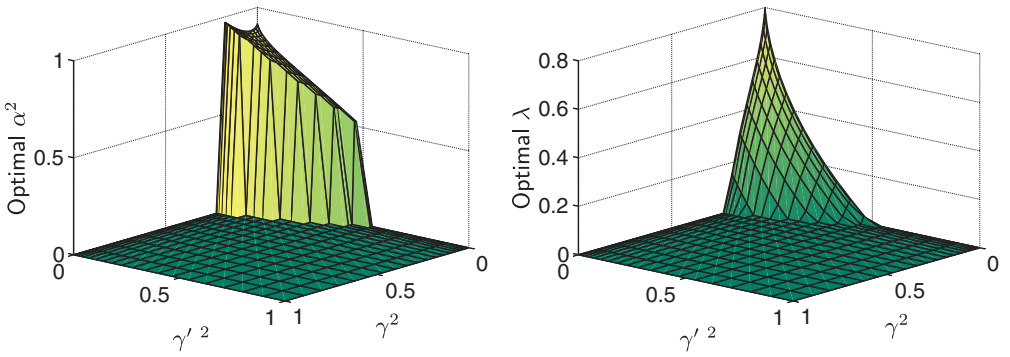

(a) (b)

FIG. 7. (Color online) Lossy asymmetric subtraction with PNRDs. (a) Optimized subtraction parameter α^2_{opt} and (b) squeezing parameter λ_{opt} under loss given asymmetric (1,0) subtraction.

This yields a log negativity of

$$E_N(\rho) = \log_2\left[\left(\frac{1-y^2}{x^2-\gamma^4\lambda^2}\right)^{t+1}\frac{P_t\left[\frac{x^2+\gamma^4\lambda^2}{x^2-\gamma^4\lambda^2}\right]}{P_t\left[\frac{1+y^2}{1-y^2}\right]}\right]. \quad (38)$$

These results reduce to the lossless symmetric detection case given by Eqs. (27) and (28) when $\gamma = \gamma' = 0$.

2. Optimizing parameters under loss

Subtraction is a general strategy for increasing entanglement. However, it is interesting to investigate which two-mode squeezed states, parameterized by λ, are most improved by this scheme. Furthermore, using Eqs. (37) and (38), we can incorporate loss as an additional input parameter. For a given implementation, the experimentalist has free choice of the reflectivity of the subtraction beam splitter (proportional to α). Therefore a logical question to ask would be, given losses of a certain level, what is the optimum range of λ for which subtraction yields the highest entanglement gain rate, and to what value should the subtraction beam splitter reflectivity be set in order to achieve this?

Figure 5(a) shows the pairs of λ and α^2 values required to produce the highest entanglement gain rate in the presence of losses. Finding an empirical fit to these data, one obtains the following formulas for setting the optimal λ and α^2:

$$\alpha_{\text{opt}}(\gamma^2) = e^{-38.1(\gamma^2+0.1)} - 0.6\gamma^2 + 0.8, \quad (39)$$

$$\lambda_{\text{opt}}(\gamma^2) = e^{-107.1(\gamma^2+0.1)^2} + e^{-2.8(\gamma^2+0.1)} - 0.2. \quad (40)$$

The gain and rate resulting from these parameters are plotted as functions of the loss parameter γ in Figs. 5(c) and 5(d), respectively. One can immediately see that there is an upper threshold on loss, above which entanglement cannot be increased.

3. Symmetric subtraction, asymmetric loss

By setting $t' = t$ in Eq. (24), one may calculate the probability of symmetric subtraction allowing for different parameters α, β, γ on each mode. However, lifting the degeneracy of the parameters across the different modes means the submatrices $\mathbf{C}^{(\mathbf{K})}$ are no longer centrosymmetric, and therefore the entanglement is not analytically tractable. Instead, we calculate numerically the entanglement from Eq. (22). Figure 6 shows the gain, probability, and rate for nondegenerate losses when subtracting a single photon from each mode. The results in Fig. 5 are simply line-outs for $\gamma = \gamma'$.

E. Losses in asymmetric subtraction

When subtracting photons asymmetrically, the effect of loss on each mode may not be equivalent. As the simplest example

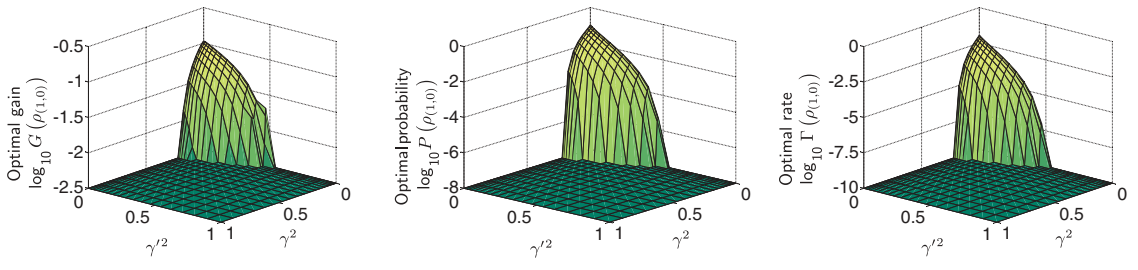

(a) (b) (c)

FIG. 8. (Color online) Lossy asymmetric subtraction using PNRDs. (a) Gain, (b) probability, and (c) rate of entanglement gain as a function of the losses γ^2, γ'^2 on modes 1 and 2, respectively. The probability of successful subtraction decreases very quickly with loss, and the positive gain region is bounded asymmetrically, being roughly twice as sensitive to losses on the unsubtracted mode.

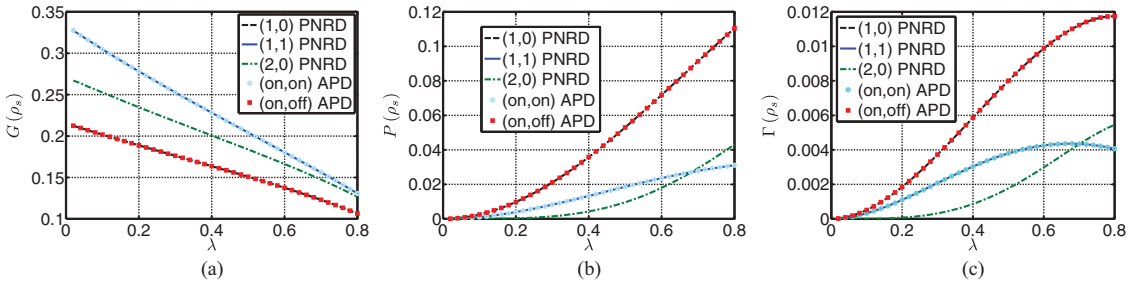

FIG. 9. (Color online) Comparing lossless subtraction strategies between APDs and PNRDs. (a) Subtraction gain, (b) probability, and (c) rate for lossless PNRDs and APDs in various subtraction strategies. The results for APDs and PNRDs for similar strategies, up to $\lambda = 0.8$, are identical.

of asymmetric subtraction, we consider the $(t,t') = (1,0)$ case, whereby one photon is subtracted from one mode, and the other mode is left unchanged. As shown in Fig. 4(c), this case produces the highest entanglement gain rate for all λ. We calculate numerically the optimal parameters $\alpha^2_{\rm opt}, \lambda_{\rm opt}$ that give the largest rate of gain, as shown in Fig. 7. Note that, since we do not subtract from the second mode, the optimal α'^2 is, trivially, $1 - \gamma'^2$ for all γ^2.

The resulting gain, probability, and rate are shown in Figs. 8(a), 8(b), and 8(c) respectively. As is to be expected, the effect of loss is not symmetric in this case. The gain region is bounded more sharply by losses in the unsubtracted mode, whereas the losses in the subtracted mode follow the scaling of the symmetric case, Fig. 5(a).

V. SUBTRACTION WITH THRESHOLD DETECTORS

We now proceed to study the enhancement of entanglement that can be effected by subtracting photons locally using threshold detectors. We consider avalanche photodiodes, detectors that click when at least one photon is incident. Starting from Eq. (22), the effect of such detectors is described by the summations over d from $t = t_{\rm max} = 0$ for "off" or from $t = 1$ to $t_{\rm max} = \infty$ for "on" and similarly for t'. This analysis can be extended to higher-photon-number threshold detectors by changing the ranges corresponding to the on and off detection. A physical example of such a detector would be a multiplexed array of n APDs with a detection event triggered off n-fold coincidences.

A. Probability of photon subtraction using APDs

The four measurement outcomes to consider when using APDs are as follows: both detectors clicking (on, on), neither clicking (off, off), or just one clicking (on, off) or (off, on). The probabilities corresponding to these events must sum to unity.

The (off, off) case is identical to the case where both PNRDs register no photons. Defining $y = (\alpha^2 + \gamma^2)\lambda, y' = (\alpha'^2 + \gamma'^2)\lambda$, the probability in this case is

$$P(\text{off, off}) = \frac{1-\lambda^2}{1-yy'}. \tag{41}$$

The (off, on) case is also analytically tractable when incorporating losses. From Eq. (24), P (off, on) is given by

$$P(\text{off, on}) = \sum_{t'=1}^{\infty} P(0,t') = \frac{(1-\lambda^2)y(\lambda - y')}{(1-y\lambda)(1-yy')}. \tag{42}$$

Note that P(on, off) is identical to the result above under exchange of primed and unprimed parameters. The probability of both detectors registering photons P(on, on) can be tackled by using the relation $\sum_{p,q=(\text{on,off})} P(p,q) = 1$, yielding

$$P(\text{on, on}) = \frac{(y-\lambda)(y'-\lambda)(1-yy'\lambda^2)}{(1-y\lambda)(1-y'\lambda)(1-yy')}. \tag{43}$$

B. Lossless subtraction

The idealized case of lossless symmetric subtraction using APDs with unit efficiency is analytically tractable [20]. However, lifting the degeneracy of the parameters means the

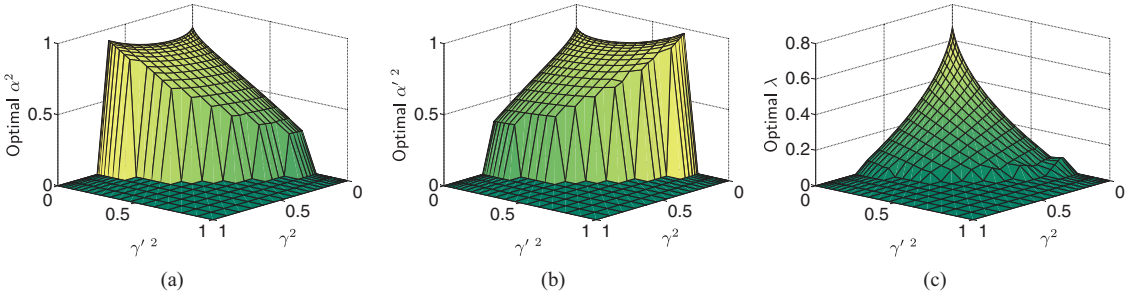

FIG. 10. (Color online) Lossy subtraction with APDs. Subtraction parameters (a) α^2 and (b) α'^2 and 10(c) squeezing parameter λ, optimized to produce the highest entanglement gain rate under loss given symmetric subtraction with APDs.

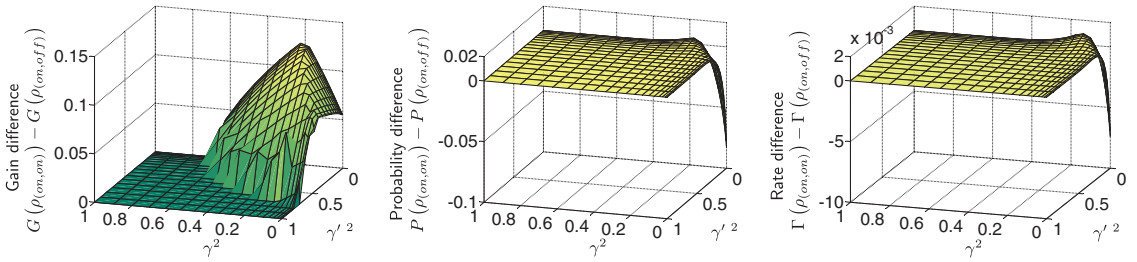

FIG. 11. (Color online) Comparing symmetric and asymmetric subtraction with APDs under loss. The difference between (on, on) and (on, off) subtraction events in (a) gain, (b) probability, and (c) rate as a function of the losses γ^2, γ'^2 on modes 1 and 2, respectively.

submatrices $\mathbf{C}_K$ are no longer centrosymmetric, rendering intractable the analytical method used previously. All subsequent results are therefore numerical.

In Ref. [20], it was shown that for squeezing parameters $\lambda < 0.95$, the results are essentially equivalent to those with PNRDs. The same is true for perfect asymmetric subtraction: the case where (1,0) photons are simultaneously detected on each mode, respectively, is, within the limits of our numerical analysis, identical to the case where (on, off) is detected with APDs, as shown in Fig. 9 up to $\lambda = 0.8$.

C. Lossy subtraction

As with the PNRD case calculated above, we can use entanglement gain rate as the figure of merit to be optimized, from which the optimal parameters can be extracted. The optimal parameters α^2_{opt} and λ_{opt} are shown in Fig. 10, with the resulting gain, probability, and rate identical to that shown for PNRDs in Fig. 8, as a function of the asymmetric loss parameters γ^2, γ'^2. Note that the optimal parameters are also the same for both the PNRD and APD cases.

1. Imperfect asymmetric detection

As with perfect subtraction, the behavior of APDs and PNRDs under loss is the same at experimentally accessible values of λ. In the lossless case, we have shown that asymmetric subtraction always produces a higher rate of entanglement gain (Sec. IV C, Fig. 8). We now ask whether one strategy is always better than the other for all losses. This turns out not to be the case, as shown in Fig. 11.

While the gain produced when subtracting from both modes is always greater than when subtracting from a single mode [Fig. 11(a)], for a particular range of losses on each mode γ, γ', the probability favors subtracting from just a single mode. This result is repeated in the plot showing the comparative rate of gain [Fig. 11(c)].

VI. CONCLUSION

We have investigated photon subtraction from a two-mode squeezed state as a means to probabilistically increase entanglement under LOCC. By defining the entanglement gain rate as our figure of merit, we are able to optimize over the subtraction beam splitter transmissivity T_2 to maximize this quantity in the presence of unequal losses on each mode. Our results may be summarized as follows.

(1) If the losses are above a threshold, which depends on the number of photons to be subtracted, local subtraction cannot enhance entanglement.

(2) When it can, (1,0) subtraction seems to be the best strategy, whether APDs or PNRDs are used to detect the subtracted photon.

(3) However, depending on how losses are distributed across the modes, symmetric subtraction may be advantageous.

(4) Subtracting more photons produces marginal enhancement in entanglement and is far less probable.

(5) APDs are essentially equivalent to PNRDs for most of the λ regime, including when accounting for asymmetric losses.

Given any realistic scenario with lossy transmission channels and imperfect detectors, our conclusions outline the most suitable strategy that must be adopted to achieve entanglement enhancement in CV systems most effectively. This approach also specifies the initial squeezing parameter λ_{opt} for which this particular protocol works best. The figure of merit we use in this paper is the entanglement gain rate, relevant to quantum communication applications. For other applications, it may be the final entanglement, or indeed the gain alone, that is more important. The methods presented in this paper can be easily modified for those purposes.

Photon subtraction is one of the simplest operations introducing non-Gaussianity, thereby opening the gate to a large class of CV quantum information processing protocols such as entanglement distillation that are not possible in the Gaussian regime. We hope that our work will inform future efforts to increase entanglement via this technique under realistic experimental conditions.

ACKNOWLEDGMENTS

The authors are grateful to M. Barbieri for useful discussions and P. van Loock for helpful correspondence. This work was supported by the Engineering and Physical Sciences Research Council of the United Kingdom (Project No. EP/H03031X/1), the US European Office of Aerospace Research and Development (Project No. 093020), the European Commission (under Integrated Project Quantum Interfaces, Sensors, and Communication based on Entanglement), and the Royal Society.

[1] C. H. Bennett, H. J. Bernstein, S. Popescu, and B. Schumacher, Phys. Rev. A **53**, 2046 (1996).
[2] P. G. Kwiat, S. Barraza-Lopez, A. Stefanov, and N. Gisin, Nature (London) **409**, 1014 (2001).
[3] J. Eisert, S. Scheel, and M. B. Plenio, Phys. Rev. Lett. **89**, 137903 (2002).
[4] J. Fiurášek, Phys. Rev. Lett. **89**, 137904 (2002).
[5] G. Giedke and J. I. Cirac, Phys. Rev. A **66**, 032316 (2002).
[6] T. Opatrný, G. Kurizki, and D.-G. Welsch, Phys. Rev. A **61**, 032302 (2000).
[7] L.-M. Duan, G. Giedke, J. I. Cirac, and P. Zoller, Phys. Rev. Lett. **84**, 4002 (2000).
[8] J. Fiurášek, L. Mišta, and R. Filip, Phys. Rev. A **67**, 022304 (2003).
[9] D. E. Browne, J. Eisert, S. Scheel, and M. B. Plenio, Phys. Rev. A **67**, 062320 (2003).
[10] E. T. Campbell and J. Eisert, Phys. Rev. Lett. **108**, 020501 (2012).
[11] E. T. Campbell, M. G. Genoni, and J. Eisert, arXiv:1211.5483 [quant-ph] (2012).
[12] B. Hage, A. Samblowski, J. Diguglielmo, A. Franzen, J. Fiurášek, and R. Schnabel, Nat. Phys. **4**, 915 (2008).
[13] R. Dong, M. Lassen, J. Heersink, C. Marquardt, R. Filip, G. Leuchs, and U. L. Andersen, Nat. Phys. **4**, 919 (2008).
[14] B. Hage, A. Samblowski, J. DiGuglielmo, J. Fiurášek, and R. Schnabel, Phys. Rev. Lett. **105**, 230502 (2010).
[15] R. Dong, M. Lassen, J. Heersink, C. Marquardt, R. Filip, G. Leuchs, and U. L. Andersen, Phys. Rev. A **82**, 012312 (2010).
[16] H. Takahashi, J. S. Neergaard-Nielsen, M. Takeuchi, M. Takeoka, K. Hayasaka, A. Furusawa, and M. Sasaki, Nat. Photonics **4**, 178 (2010).
[17] P. T. Cochrane, T. C. Ralph, and G. J. Milburn, Phys. Rev. A **65**, 062306 (2002).
[18] S. Olivares, M. G. A. Paris, and R. Bonifacio, Phys. Rev. A **67**, 032314 (2003).
[19] A. Kitagawa, M. Takeoka, M. Sasaki, and A. Chefles, Phys. Rev. A **73**, 042310 (2006).
[20] S. L. Zhang and P. van Loock, Phys. Rev. A **82**, 062316 (2010).
[21] C. Navarrete-Benlloch, R. Garcia-Patron, J. H. Shapiro, and N. J. Cerf, Phys. Rev. A **86**, 012328 (2012).
[22] M. S. Kim, J. Phys. B **41**, 133001 (2008).
[23] G. Adesso, Phys. Rev. A **79**, 022315 (2009).
[24] A. Ourjoumtsev, A. Dantan, R. Tualle-Brouri, and P. Grangier, Phys. Rev. Lett. **98**, 030502 (2007).
[25] M. B. Plenio, Phys. Rev. Lett. **95**, 090503 (2005).
[26] A. Peres, Phys. Rev. Lett. **77**, 1413 (1996).
[27] M. Horodecki, P. Horodecki, and R. Horodecki, Phys. Lett. A **223**, 1 (1996).
[28] S. L. Braunstein and P. van Loock, Rev. Mod. Phys. **77**, 513 (2005).
[29] M. A. Nielsen, Phys. Rev. Lett. **83**, 436 (1999).
[30] National Institute of Standards and Technology, Digital Library of Mathematical Functions, http://dlmf.nist.gov/26.4.
[31] A. Cantoni and P. Butler, Linear Algebra Appl. **13**, 275 (1976).
[32] J. Eisert, F. G. S. L. Brandão, and K. M. R. Audenaert, New J. Phys. **9**, 46 (2007).